



Dynamical structure of peptide molecules: Fourier transform microwave spectroscopy and *ab initio* calculations of *N*-methylformamide

Yoshiyuki Kawashima^{a,*}, Tsuyoshi Usami^a, Richard D. Suenram^{b,c}, G. Yu. Golubiatnikov^{b,1}, Eizi Hirota^d

^a Department of Applied Chemistry, Kanagawa Institute of Technology, Atsugi, Kanagawa 243-0292, Japan

^b Optical Technology Division, National Institute of Standards and Technology, Gaithersburg, MD 20899-8441, USA

^c Department of Chemistry, University of Virginia, McCormick Rd., Charlottesville, VA 22904-4319, USA

^d The Graduate University for Advanced Studies, Hayama, Kanagawa 240-0193, Japan

ARTICLE INFO

Article history:

Received 4 May 2010

In revised form 8 June 2010

Available online 17 June 2010

Keywords:

Peptide linkage molecule
Fourier transform microwave spectroscopy
Isotopomer
Molecular structure
Internal rotation

ABSTRACT

Rotational spectra of both *trans* and *cis* forms of the *N*-methylformamide normal as well as deuterated (HCONDCH₃, referred to as N–D) species were observed by Fourier transform microwave spectroscopy in the frequency region from 5 to 118 GHz. Samples were prepared in the form of a beam by a pulsed jet valve maintained at 50 °C and were introduced in a high-vacuum cavity cell, with either Ne or Ar as a carrier gas at a backing pressure of 100 kPa. The observed spectra were analyzed to yield molecular parameters including rotational constants and barrier, V_3 , to CH₃ internal-rotation: 53.9 (6) and 301 (4) cm^{−1} for the *trans* and *cis* forms of the normal species, respectively, and 41.9 (6) and 309 (4) cm^{−1} for the *trans* and *cis* forms of the N–D species, respectively. Spectra of four *trans* isotopologues with ¹³C, ¹⁵N, or ¹⁸O singly-substituted in the internal-rotation *A* state were observed and analyzed to derive the r_s structure of the *trans* form. For comparison with the experimental data, *ab initio* calculations were carried out at MP2/6-31G** level to derive molecular structure, potential barrier to CH₃ internal rotation, and the energy difference between the *cis* and *trans* forms. An extensive coupling was found between the CH₃ internal rotation and N–H out-of-plane bending, suggesting that the potential function for the CH₃ internal-rotation deviates considerably from a simple cos(3α) form. The effects of the V_6 term is briefly discussed.

© 2010 Elsevier Inc. All rights reserved.

1. Introduction

Peptide molecules refer to those species which contain one (or more) peptide linkage(s) as a central backbone and are, in the simplest cases, represented by the chemical formula: XCO–NH₂ shown in Fig. 1. They have attracted much attention, primarily because of the important roles they play in various biological systems. Fortunately, some of them can be vaporized without too much decomposition so that a workable sample exists as single molecules in the gas phase. Their molecular structure has thus been explored in detail by spectroscopic methods such as infrared and nuclear magnetic resonance. Our group has been applying Fourier transform microwave (abbreviated as FTMW) spectroscopy to a few peptide molecules, as reviewed in Ref. [1], where our earlier results are summarized.

N-methylformamide HCONHCH₃ (hereafter abbreviated as NMFA) is one of the most important peptide molecules; although it is quite simple in structure, it bears several interesting characteristics

representative of peptide molecules. It is formed when X is H and Y is CH₃ in Fig. 1. According to a convention widely accepted, we shall call the conformation *trans*, when X and Y are on the opposite side of the central C–N bond and *cis*, when they are on the same side. In the *cis* form, we will replace Y with Y' in order to stress the difference in conformation. In view of the important roles in science in general played by NMFA, we decided to study this molecule by FTMW, aiming at deep understanding at a molecular level of characteristic behaviors of this and related species in various fields.

NMFA was known to exist in *trans* and *cis* forms in the liquid and solution phases, but there was some controversy as to the most stable conformer in the gas phase. Jones [2] observed a few infrared bands in the gas phase and concluded most of them were consistent with the *cis* form, except for a band at 1280 cm^{−1}. However, Miyazawa [3] and later Suzuki [4] performed detailed analyses of normal coordinates and showed that most infrared bands were due to the *trans* form, contrary to the conclusion of Jones. Miyazawa assigned the 1280 cm^{−1} band, which Jones mentioned as an exceptional *trans* band, to the C–N stretching band of *cis*. Later Hallam and Jones [5] introduced a long-path (40 m) cell in their infrared spectrometer and measured the *P*–*R* separations for the C=O stretch, amide III, and N–CH₃ stretching bands and also

* Corresponding author. Fax: +81 46 242 8760.

E-mail address: kawashima@chem.kanagawa-it.ac.jp (Y. Kawashima).

¹ Permanent address: Institute of Applied Physics, Russian Academy of Science, Ulanov Street 16, 603600 Nishnii Novgorod, Russia

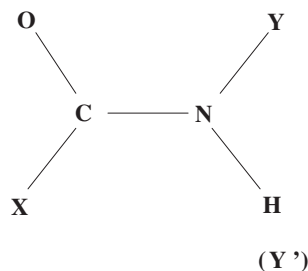


Fig. 1. Schematic diagram of the peptide molecule.

for the band at 1280 cm^{-1} , with much higher accuracy than Jones did. They thus definitely concluded that the former three bands were ascribed to *trans* and the last one to *cis*, in agreement with Miyazawa, thereby establishing that NMFA exists predominantly in the *trans* form also in the gas phase. More recently, Sugawara et al. [6] observed a band at 578 cm^{-1} at the resolution of 0.12 cm^{-1} and derived rotational constants, in good agreement with those expected for the *cis* form. They assigned this band to the N–H out-of-plane bending of the *cis* form. According to Suzuki, the corresponding band of *trans* form was observed at 720 cm^{-1} .

Proton nuclear magnetic resonance (NMR) spectroscopy was also employed extensively to determine the abundance ratio of the two conformers of NMFA, *trans* and *cis*, in the liquid and solution phases [7,8]. The *cis/trans* ratio reported ranges from 11/89 to 5/95 at room temperature. Dorman and Bovey [9] and Nakanishi and Roberts [10] extended the method to ^{13}C and ^{15}N resonances and demonstrated that these signals were useful not only in determining the *cis/trans* abundance ratio, but also in elucidating the conformations of peptides as a whole. Kitano and Kuchitsu [11] investigated NMFA by electron diffraction and determined the molecular structure (r_g and θ_α) of the *trans* form, but they failed to detect the *cis* form. A most recent study of NMFA by IR, NMR and *ab initio* calculations should also be mentioned [12]; the authors concluded that the *cis* form was present also in the gas phase up to about 5%.

During 1960s and 1970s, several groups attempted to assign the microwave spectra of NMFA without success. It was 1996 that Fantoni and Caminati [13] reported the first successful microwave study of NMFA; they assigned spectra of the *trans* form in the CH_3 internal-rotation state of *A* symmetry, but could not identify spectral lines of the *E* state and thus estimated the internal-rotation potential barrier by using the pseudo-inertial defect Δ defined by $\Delta = I_{cc} - I_{aa} - I_{bb} + 2\sum_i m_i c_i^2$, where c_i denotes the out-of-plane coordinate of the *i*-th atom, in conjunction with *ab initio* calculations. Their measurements covered spectra of both the parent and HCONDCH_3 (hereafter abbreviated as N–D) species. Later Fantoni et al. [14] published the observation and the analysis of *E* lines and reported the barrier V_3 to CH_3 internal rotation to be $55.17(84)\text{ cm}^{-1}$.

FTMW spectroscopy is normally combined with a molecular beam generated by introducing a high-pressure sample through a pulsed jet valve into a high-vacuum cavity cell of the spectrometer. This method allows us to lower the rotational temperature of molecules in the beam to a few Kelvin, thereby simplifying the rotational spectra. This is a great advantage and it is particularly applicable to a molecule with low-frequency internal modes. However, at the same time this advantage can become a drawback; when the molecule to be studied relaxes by jet expansion to a lowest eigenstate, we lose all the information that can be extracted from spectra of excited states. A few exceptions to this sort of relaxation are known; when some “excited” states, i.e. high-energy eigenstates belong to symmetry different from that of the ground, i.e. lowest-energy state, molecules can survive in these excited states even in a molecular beam as cold

as a few Kelvin. The other type of exception has been reported for a system in which a high barrier hinders molecules to make transitions from higher energy states to lower energy states. How many molecules then remain in excited states seems to depend on the form of the potential barrier, energy difference, and other molecular properties. It is interesting to examine how the two conformers, *cis* and *trans*, of NMFA behave in this respect. According to our *ab initio* calculations, the energy difference between *cis* and *trans* is as large as 466 cm^{-1} . Therefore, the observation of *cis* spectra would be impossible, if molecules easily surpass the barrier between the two conformations during the process of jet cooling. It is thus challenging for us to try to detect *cis* spectra and, once observed, they will give us invaluable information on the conformational change of this important peptide molecule NMFA.

We have also shown by an *ab initio* calculation that the CH_3 internal rotation is closely coupled with the N–H out-of-plane bending mode. It would thus be interesting to detect spectra of the N–D species in the *E* internal-rotation state and to derive the potential barrier V_3 for this species, which might provide us with further information on the coupling between the CH_3 internal rotation and the N–H out-of-plane bending and on the origin of V_3 . In this respect, we should mention our recent study of acetamide by FTMW spectroscopy [15]. This molecule has been known to have an extremely low V_3 : 25.043857 cm^{-1} [16], and we have traced the origin of this low barrier by examining the effect of deuterium substitution in the amino group. In this process we found that the amino wagging motion is coupled with the CH_3 internal rotation to result in an abnormally large V_6 term of $-10.044874\text{ cm}^{-1}$ [16]. This result makes it sensible for us to study the N–D species of NMFA as well, namely we may expect that this species will provide us with information on the internal motions of NMFA.

We should add that the important roles of NMFA in many fields have prompted many theoretical calculations to be carried out. Here, a few recent publications are cited to show a variety of approaches [17–19].

2. Experimental methods and *ab initio* calculations

Two Fourier transform microwave spectrometers were employed in the present study, one at NIST (National Institute of Standards and Technology) [20] and the other at KAIT (Kanagawa Institute of Technology) [21]. The latter was originally designed after the NIST spectrometer, but has been improved to cover wider frequency region. At an initial stage of the present study, we scanned the frequency region from 10 to 25 GHz using the NIST spectrometer. Later we expanded the region: the lowest limit down to 4 GHz and the highest up to 36 GHz by using the KAIT spectrometer. In these spectrometers the molecular beam was produced through a 0.9 mm diameter nozzle attached to a pulsed valve (General Valve Series 9) and oriented parallel to the cavity axis. With this type of spectrometer, frequency measurements are generally accurate to about 4 kHz. Samples of NMFA, which were commercially available, were used without further purification. The deuterated (N–D) species was prepared by a proton/deuterium exchange reaction of the NH group in HCONHCH_3 and OD in CD_3OD . The spectrum of the N–D species was observed in the region between 4 and 36 GHz. The samples heated to about 50°C were introduced into the cell with either Ne or Ar as a carrier gas at the backing pressure of about 100 kPa. We did not observe any indication of the sample being thermally decomposed at this temperature. The rotational temperature of the beam thus generated was typically 3 K under these conditions. The absorption signal was accumulated 100–1000 times in order to obtain a good signal-to-noise ratio.

Additional measurements were performed to detect some $J=4-3$ transitions of the *E* state of the *trans* form around

43 GHz region, using a Fourier transform microwave spectrometer [22] set up at the Department of Physics, The University of Tokyo, by the courtesy of Professor Satoshi Yamamoto and Ms. E. Kim. The observation was also extended to millimeter-wave region from 58 to 118 GHz, by using another spectrometer of NIST, which employed a precision-tunable KVARZ millimeter synthesizer with an output power of about 10 mW as a source [23]. The millimeter waves passed through a jet-cooled beam of sample generated in a similar way as in the other spectrometers and was focused on a high sensitivity liquid-He cooled hot electron bolometer (QMC). The signal-to-noise ratio and the line width thus achieved allowed us to measure the frequency of a millimeter-wave line to an uncertainty of 10 kHz. However, sometimes the line shape was observed distorted, reducing the precision of frequency measurements to 50 kHz or so.

We performed *ab initio* molecular orbital calculations using the Gaussian 98 program package [24]. Molecular geometry was derived both for *trans* and *cis* forms by second-order Møller–Plesset perturbation theory (MP2) [25] with a 6–31G** basis set [26].

3. Observed spectra and analysis

3.1. *Trans* form of the normal and N–D species

As mentioned in Section 1, Fantoni and Caminati [13] observed the *A*-state spectrum of the normal and N–D species of NMFA in the region between 18 and 40 GHz, and later Caminati and his co-workers [14] extended the measurements on the normal species to the millimeter-wave region up to nearly 80 GHz. We scanned the frequency region down to 5 GHz and added a few low-*J* transitions including $1_{01} \leftarrow 0_{00}$. Our measurements are of much higher resolution and precision than those of Caminati et al., thanks to the Fourier transform method combined with the beam technology, allowing us to resolve the nitrogen nuclear quadrupole hyperfine structure almost completely. We thus obtained spectral data of the *trans* *A* state, much improved in accuracy and scope from those of Fantoni and Caminati.

As Fantoni et al. [14] have reported, the rotational selection rule for the internal-rotation *E* state is relaxed such that only the $\Delta J = 0$ and ± 1 rules remain to hold, and each rotational state is better designated by a signed *k* quantum number, which is conserved in a symmetric top, rather than by the asymmetric-rotor $K_a K_c$ representation. In assigning the observed spectra we relied on sum rules among transition frequencies. The nitrogen nuclear quadrupole hyperfine structure was also quite helpful as an aid to spectral assignment.

We started searching for *E* state spectra with the detection of $J, k = 1, 0 \leftarrow 0, 0$, which corresponds to the $1_{01} \leftarrow 0_{00}$ transition in the *A* state. After careful scanning, we detected a triplet centered at 9659.742 MHz. Then we progressed step-by-step, based on sum rules and hyperfine patterns, as already mentioned, and assigned transitions among rotational levels of $J = 0, 1$, and 2 and $k = 0, +1$, and -1 . Detection and assignment were much more difficult to make for levels with $|k| \geq 2$, because not many lines were observed in the frequency region covered. In this respect, the measurements in the millimeter-wave region were of great help. We covered more than 80% of the region from 58 to 118 GHz and observed 93 lines, of which 46 lines were assigned to the *trans* *A* state and another 46 lines to the *trans* *E* state, leaving one line unassigned. Caminati and his collaborators [14] observed 28 lines in the millimeter-wave region, nine of which overlapped with our lines, but others were not on our list, probably because the effective temperature of their experiment was much higher than ours and also because of mode gaps intrinsic in the NIST spectrometer. Table 1 lists the observed frequencies and observed minus calculated values for a few lowest transitions of $J = 1 \leftarrow 0$ and $1 \leftarrow 1$,

for the *trans* form. A complete list of the observed and calculated transition frequencies for the *trans* form of NMFA is available as electronic supplementary information, Table S-1.

We searched for *A* and *E* state spectra of the N–D species as in the case of the normal species, namely starting with the detection of the $1_{01} \leftarrow 0_{00}$ *A*-state line and the *E*-state line of $J, k = 1, 0 \leftarrow 0, 0$; we finally detected the latter at 7962, 3114 MHz lower than the *A* line, which should be compared with 1648 MHz for the normal species. The difference is ascribed to the fact that the V_3 of the N–D species is effectively lower than that of the normal species. We then searched other spectra in the region from 4 to 36 GHz and finally observed and assigned 36 transitions for both *A* and *E* states of the *trans* N–D species, based upon the sum rule and *eQq* splitting patterns. We did not try to resolve and measure the deuterium hyperfine structure, and thus the accuracy of the frequency measurements was somewhat lower for the N–D species than for the normal species. Some of the observed low-*J* transitions are listed in Table 1, while all the observed transitions are included in Table S-1 (electronic supplementary information).

For the analysis of the observed spectra, we employed the Hamiltonian and the computer program, which we developed previously, based on a rho-axis method [27], to analyze the rotational spectra of *N*-methylpropionamide [28]. We have, however, slightly modified the program, by explicitly introducing the sum rule for the direction cosines of the methyl internal-rotation axis with respect to the principal axes of inertia. We have employed only the data obtained by FTMW spectroscopy, because of much higher reliability of these data than those by millimeter-wave spectroscopy.

We analyzed the observed frequencies of the normal species in both the *A* and *E* states simultaneously and could reproduce them with the standard deviation of 24 and 14 kHz for the normal and N–D species, respectively. Molecular parameters thus derived are listed in Table 2. When the moment of inertia of the methyl top was increased by $0.04 \mu\text{Å}^2$, the potential barrier V_3 to methyl internal rotation was changed from $53.91824(11)$ to $53.30337(9) \text{ cm}^{-1}$, while other parameters changed little. We thus concluded that the internal-rotation potential barriers V_3 of the *trans* normal and N–D species of NMFA were $53.9(6)$ and $41.9(6) \text{ cm}^{-1}$, respectively, where the uncertainty was mainly due to that in the CH_3 moment of inertia, $\pm 0.04 \mu\text{Å}^2$. This result agrees quite well with that of Fantoni et al. on the normal species $55.17(84) \text{ cm}^{-1}$ [14], but care should be taken in comparing the two sets of the results, because the molecular model employed is quite different.

We have calculated the intensities of *E* lines, by using the dipole moment components, which we derived by the *ab initio* method described in a previous section. We could reproduce the observed intensities of *E* lines qualitatively, in spite of the fact that *E* levels are mixed extensively within a *J* manifold by the two following factors of quite different nature, molecular asymmetry and first-order contributions of internal rotation. The former tends to split $|k|$ degenerate levels by $\Delta k = \pm 2$ matrix elements, whereas the latter tends to make $+k$ and $-k$ levels repel each other by the opposite internal-rotation contributions to them. Fig. 2 shows how the *E* energy level structure differs from the corresponding *A* level structure for a few low-*J* manifolds.

3.2. *Trans* isotopomers in the *A* state

In order to determine the molecular structure of NMFA, we observed spectra of the ^{13}C , ^{15}N and ^{18}O isotopomers in natural abundance. For ease of detecting and analyzing the spectra, we limited the observations to the *trans* form in the *A* internal-rotation state, i.e. to four *a*-type and four *b*-type transitions for each of the four isotopomers, as listed in Table 3. These spectra were analyzed by a conventional asymmetric-top rotational Hamiltonian to derive rotational, centrifugal distortion, and nitrogen nuclear quadrupole

Table 1
Observed frequencies and their deviations from the calculated frequencies of rotational transitions of *trans* normal and N-D species of NMFA (in MHz).

Transition									Normal species		N-D species	
<i>A state</i>												
<i>F'</i>	<i>J'</i>	<i>K'_a</i>	<i>K'_c</i>	–	<i>F''</i>	<i>J''</i>	<i>K''_a</i>	<i>K''_c</i>	Obs ^a	O–C ^b	Obs ^a	O–C ^b
2	1	0	1	–	1	0	0	0	11307.5486	–6.2	11076.8869	7.2
1	1	0	1	–	1	0	0	0	11308.1169	–4.2	11077.4516	4.4
0	1	0	1	–	1	0	0	0	11306.6912	–14.1	11076.0287	0.2
2	1	1	1	–	1	0	0	0	24888.5842	–4.9	23103.0460	–2.7
1	1	1	1	–	1	0	0	0	24889.2268	–5.6	23103.7141	9.1
0	1	1	1	–	1	0	0	0	24887.6193	–4.9	23102.0697	5.4
2	1	1	0	–	2	1	0	1	15083.3820	–5.3	13614.9666	0.0
2	1	1	0	–	1	1	0	1	15082.8117	–9.2	13614.4020	2.9
1	1	1	0	–	2	1	0	1	15082.1730	–4.7	13613.7332	–9.6
1	1	1	0	–	1	1	0	1	15081.6047	–6.6	13613.1686	–6.8
1	1	1	0	–	0	1	0	1	15083.0285	1.3	13614.5916	–2.4
0	1	1	0	–	1	1	0	1	15084.6301	–5.2	13616.2294	–5.3
<i>E state</i>												
<i>F'</i>	<i>J'</i>	<i>k'</i>		–	<i>F''</i>	<i>J''</i>	<i>k''</i>					
2	1	0		–	1	0	0		9659.7420	25.0	7962.1889	–33.6
1	1	0		–	1	0	0		9660.0584	23.2	7962.3255	–26.0
0	1	0		–	1	0	0		9659.2660	26.3	7962.0012	–27.5
2	1	1		–	1	0	0		16856.2539	26.8	15208.3003	17.4
1	1	1		–	1	0	0		16856.3154	22.1	15208.5433	–0.7
0	1	1		–	1	0	0		16856.1563	28.6	15207.8862	–5.1
2	1	–1		–	1	0	0		34162.8069	1.0	–	–
1	1	–1		–	1	0	0		34162.4214	–0.1	–	–
0	1	–1		–	1	0	0		34163.3775	–5.1	–	–
2	1	–1		–	2	1	0		24503.0605	–28.4	26063.6907	27.3
2	1	–1		–	1	1	0		24502.7461	–24.6	26063.5798	45.5
1	1	–1		–	2	1	0		24502.6817	–22.8	26063.3057	32.5
1	1	–1		–	0	1	0		24503.1474	–34.4	–	–
0	1	–1		–	1	1	0		24503.3198	–27.6	26064.1392	19.6
1	1	–1		–	1	1	0		24502.3639	–22.4	26063.1716	27.4
2	1	–1		–	2	1	1		17306.5484	–30.4	18817.6100	7.1
2	1	–1		–	1	1	1		17306.4957	–16.9	18817.3486	6.7
1	1	–1		–	2	1	1		17306.1099	–84.6	18817.2143	1.5
1	1	–1		–	0	1	1		17306.2662	–27.7	18817.6100	5.6
0	1	–1		–	1	1	1		17307.0684	–21.0	18817.9193	–7.9
1	1	–1		–	1	1	1		17306.1099	–18.3	18816.9615	9.8

^a In MHz.^b In kHz.

coupling constants, as listed in Table 4. Because only eight transitions were employed, Δ_K and δ_K were fixed to the values of the normal species. The corresponding spectra of the normal and N-D species were treated in the same way, as shown in Table 4, where the spectral data of the N-D species were taken from Ref. [13].

3.3. *Cis* form of the normal and N-D species

Because the *cis* form is a near prolate symmetric top with a large *a* component of dipole moment, it was quite easy to identify *a*-type, *R*-branch transitions. The $1_{01} \leftarrow 0_{00}$ transition of the *A* internal-rotation state was assigned to a triplet centered at 8484.276 MHz; the hyperfine structure well conformed to the pattern expected for a $J = 1 \leftarrow 0$ transition. This triplet was found partially overlapped by another triplet of similar pattern centered at 8483.300 MHz, which was ascribed to the *E* internal-rotation state. We then extended the observation up to $J = 3 \leftarrow 2$ without difficulty. The intensity of these *cis* lines relative to that of *trans* was found close to that expected for the abundance of the two conformers at 50 °C. We tried hard to observe *b*-type transitions for *cis* form without success. Our *ab initio* calculation yields the components of the dipole moment to be $\mu_a = 4.45$ D, $\mu_b = 0.45$ D, and $\mu_c = 0.007$ D, and thus we expect that *b*-type lines are two orders of magnitude weaker than *a*-type lines, which explains our failure to detect *b*-type lines. Some of the observed frequencies and observed minus calculated values for a few lowest *J* transitions up to $J = 3 \leftarrow 2$ of the *cis* normal and N-D species were listed in Table 5. Fig. 3 shows the $J = 2 \leftarrow 1$ transition of the *cis* form observed for the *A* and *E* states of the normal and

N-D species. A complete list of the observed and calculated transition frequencies of the *cis* normal and N-D species of NMFA is available as electronic supplementary information, Table S-5.

We analyzed the observed spectra of both *A* and *E* states simultaneously, by taking the *A* and *B* rotational constants common to the internal-rotation *A* and *E* states, while including the *D* constants in the parameter set. The *A* constant of the N-D species was fixed to an appropriate value, because the observed spectra were limited in number. Molecular constants thus derived are given in Table 6. When the moment of inertia of the methyl top decreased by $0.076 \text{ u}\text{\AA}^2$, the potential barrier V_3 to methyl internal rotation increased from $300.791 (48)$ to $304.423 (52) \text{ cm}^{-1}$, but other parameters were little changed. We have concluded that the internal-rotation potential barrier V_3 of the *cis* normal and N-D species of NMFA were $301 (4)$ and $309 (4) \text{ cm}^{-1}$, respectively, again with the uncertainty being estimated mainly to be due to that in the CH_3 moment of inertia. Because of the high methyl internal-rotation potential barrier V_3 , no higher-order terms were required in fitting the observed spectra of the *cis* form, in sharp contrast with the case of the *trans* form.

4. Discussion

4.1. Detection of both *trans* and *cis* forms in relation to the structure of the peptide linkage

We have succeeded in observing the rotational spectra of both *trans* and *cis* N-methylformamide. Although the *cis* form is *ab initio*

Table 2

Molecular constants of the *trans* normal and N-D species of NMFA^a. The rho-axis method is used.

Constant	Normal species	N-D species
A state		
A _{RAM}	17149.7253 (51)	15277.5107 (46)
B _{RAM}	8603.9956 (28)	8813.2983 (26)
C	4902.4412 (25)	4744.2815 (27)
Δ _J	0.13995 (48)	0.24468 (28)
Δ _{JK}	−1.5610 (48)	−2.1367 (16)
Δ _K	2.2702 (72)	2.245 ^b
δ _J	0.06851 (22)	0.12130 (19)
δ _K	−0.22597 (90)	−0.2855 (12)
E state		
A _{RAM}	17342.174 (93)	15568.268 (11)
B _{RAM}	8329.4485 (82)	8433.2460 (61)
C	4907.868 (59)	4751.6273 (39)
Δ _J	0.063 (13)	0.23561 (51)
Δ _{JK}	−0.54 (13)	−1.6355 (29)
Δ _K	0.81 (16)	0.9663 ^b
Δ _J	0.0350 (75)	0.06996 (25)
δ _K	−0.237 (48)	−0.3067 ^b
N-CH₃		
V ₃	53.91824 (11)	41.903365 (12)
I _α	3.1542735 ^b	3.182312 ^b
λ _a	0.90814582 ^b	0.881281 ^b
ρ _a	0.0768384 ^b	0.0694099 ^b
Δ _{EKJ}	1.047 (96)	1.1819 ^b
Δ _{EKK}	2.026 (98)	1.8663 ^b
Δ _{EKK}	−10.84 (20)	−9.8071 ^b
Δ _{EXX}	0.0 ^b	0.0 ^b
Δ _{EKK}	0.298 (79)	0.4237 ^b
Δ _{EXJ}	0.0 ^b	0.0 ^b
δD _E	287.323 (73)	318.9787 (24)
D _E	−5002.757 ^b	−4865.7 ^b
χ _{aa}	2.115 (22)	2.148 (10)
χ _{bb} − χ _{cc}	5.952 (28)	6.011 (16)
χ _{ab}	0.265 (17)	0.2619 (67)
A _{PAM}	19455.9905	17886.7697
B _{PAM}	6297.7305	6204.0393
σ	0.0245	0.0138

^a In MHz, except for V₃ which is given in cm^{−1}, I_α in uÅ², and λ_a and ρ_a, which are dimensionless. Values in parentheses denote standard deviations given in the last digits of the constants.

^b Fixed; I_α was adjusted to achieve a best fit.

calculated at the MP2/6-31G** level to be higher in energy than *trans* by 466 cm^{−1}, the observed *cis* spectra were quite strong compared with the *trans* spectra, much stronger than expected from the energy difference. This observation suggests that the barrier to internal rotation about the central C–N bond is quite high, so that molecules in the *cis* potential minimum are effectively trapped there during the supersonic-jet cooling process, *i.e.* they are not further relaxed to the lowest minimum of the *trans* form. Recently we have detected both *trans* and *cis* forms also for *N*-ethylformamide (NEFA) [29]. The energy difference between the two forms was calculated by an *ab initio* method at the MP2/6-31G** level to be 179 cm^{−1}, much smaller than that of *N*-methylformamide, and in fact, the spectra of *cis* *N*-ethylformamide were observed almost as strong as those of *trans*.

4.2. CH₃ internal-rotation potential barrier

The potential barrier, V₃, of the *trans* form, 53.9 (6) cm^{−1}, is quite low, even lower than those for CH₃ in the Y position of two other peptide molecules: 83.2 cm^{−1} in CH₃CONHCH₃ [30] and 80.1 cm^{−1} in CH₃CH₂CONHCH₃ [28]. This low V₃ value may be ascribed to the electronic configuration of the C–N–H group when viewed from CH₃ in the Y position; it may look like those of aromatic molecules, in which V₃ for a CH₃ attached to the aromatic ring is often very close to zero, or vanishes completely as in the case of the benzene ring, because of C_{2v} symmetry.

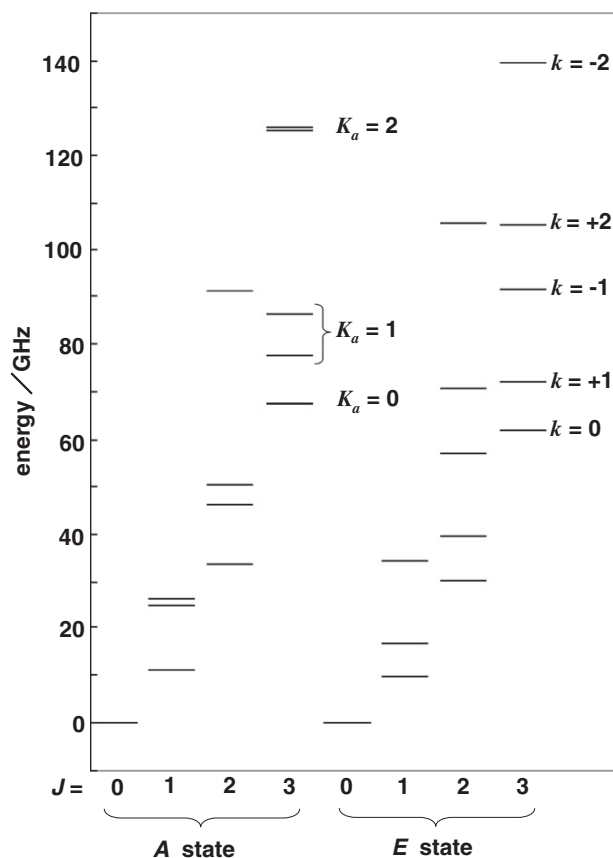


Fig. 2. Rotational energy levels of the *trans* form normal species of NMFA.

The V₃ value for the *cis* form is 5.6 times larger than that of the *trans* form. The methyl group of the *cis* form is also attached to the C–N–H group, but probably the electronic configuration is quite different from that of the *trans* form. In this respect, the results on *N,N*-dimethylformamide reported by Heineking and Dreizler [31] are interesting. There, the V₃ value is quite different for the two CH₃ groups: 366 and 772 cm^{−1} for the *trans* (Y) and *cis* (Y') positions, respectively. Both of these barriers are much higher than the corresponding ones of NMFA, and the *cis/trans* barrier ratio of 2.1, although not as large as that of NMFA, is much larger than 1.

We have examined the effects of other internal motions on the methyl internal rotation. The most conspicuous one encountered was the N–H out-of plane bending mode. Fig. 4 shows a two-dimensional potential functions of the *trans* and *cis* forms, calculated by the *ab initio* method described in a previous section, where the abscissa and the ordinate represent the CH₃ internal rotation and N–H out-of plane bending coordinates, respectively. As indicated by closed circles in Fig. 4a and b, the lowest-energy path deviates considerably from the internal-rotation coordinate axis. At equilibrium, *i.e.* in the lowest-energy conformation, one of the C–H bonds of the methyl group eclipses the central C–N bond and the two bonds move in opposite way, namely one bond moves above the molecular plane, whereas the other dives below the plane. When the CH₃ group rotates, approaching 45°, the N–H out-of plane angle is bent away from the molecular plane by as much as 13°, in the *trans* form. This trend is even more conspicuous in the *cis* form where the N–H bond is bent out of the plane by as much as 24°. In this respect it would be worth mentioning that the NH₂ out-of plane mode of formamide was shown to have an abnormally large quartic character in its potential function, although the molecule is completely planar at the equilibrium

Table 3Observed frequencies and their deviations from the calculated frequencies of rotational transitions of the *trans* A state of the isotopic species of NMFA (in MHz).

Transition										H ¹³ CONHCH ₃		HC ¹⁸ ONHCH ₃		HCO ¹⁵ NHCH ₃		HCONH ¹³ CH ₃		
J'	K' _a	K' _c	–	J''	K'' _a	K'' _c	F'	–	F''	Obs ^a	O–C ^b	Obs ^a	O–C ^b	Obs ^a	O–C ^b	Obs ^a	O–C ^b	
a-type																		
1	0	1	–	0	0	0	2	–	1	11222.1875	3.9	10850.1180	6.3	}	11246.4499	2.8	11027.3660	2.9
							1	–	1	11222.7567	1.8	10850.6649	–10.8				11027.9384	3.8
							0	–	1	11221.3301	3.3	10849.2702	4.5				11026.5075	1.5
2	0	2	–	1	0	1	3	–	2	22326.8609	2.2	21592.7417	0.8	}	22371.2260	1.3	21945.6350	1.2
							2	–	2	22327.5711	–0.9	21593.4420	0.2				21946.3430	–0.5
							2	–	1	22327.0054	4.6	21592.8775	–0.3				21945.7736	1.6
							1	–	1	22325.8949	3.7	21591.7832	–4.3				21944.6689	0.9
							1	–	0	22327.3228	3.5	21593.2010	3.6				21946.0989	2.3
2	1	2	–	1	1	1	3	–	2	20950.6199	1.1	20278.6339	1.7	}	20981.8509	1.6	20610.8395	1.6
							2	–	2	20951.9127	–3.1	20279.9234	3.5				20612.1400	4.2
							2	–	1	20951.2791	2.6	20279.2839	1.9				20611.4982	2.3
							1	–	1	20949.2613	2.3	20277.2686	–13.0				20609.4769	–0.1
							1	–	0	20950.8592	2.0	20278.8768	3.2				20611.0734	–3.4
2	1	1	–	1	1	0	3	–	2	23936.5461	–4.8	23120.4361	0.7	}	24002.2098	–2.8	23497.1450	–0.8
							2	–	2	23935.8620	–4.0	23119.7420	–9.9				23496.4521	–8.1
							2	–	1	23937.0769	0.4	23120.4361	0.7				23497.6707	–0.8
							1	–	2	23936.9262	–5.2							
							1	–	1	23938.1412	–0.7	23122.0271	10.1				23498.7368	–1.2
							1	–	0	23935.1118	–3.5	23119.0107	–1.6				23495.7106	0.9
b-type																		
1	1	1	–	0	0	0	2	–	1	24671.8556	1.2	}	24534.9208	–2.8	24595.5461	–1.2		
							1	–	1	24672.4889	–4.8						24596.1810	–6.2
							0	–	1	24670.8900	–5.5						24594.5868	–0.7
1	1	0	–	1	0	1	2	–	2	14942.9543	2.1	}	14798.7281	2.9	15011.6510	2.8		
							1	–	2	14941.7400	–1.7						15010.4390	2.1
							2	–	1	14942.3810	0.0						15011.0771	0.3
							1	–	1	14941.1713	0.9						15009.8668	1.3
							0	–	1	14944.1961	–0.6				14812.0000	–33.5	15012.8929	–0.9
							1	–	0	14942.5980	–0.5				14810.4398	1.1	15011.2951	1.0
2	1	1	–	2	0	2	3	–	3	16552.6421	–2.3	}	16429.7119	–0.0009	16563.1578	–2.5		
							2	–	3	16551.9646	5.2						16562.4744	–0.3
							3	–	2	16551.9236	–7.5						16562.4480	–2.6
							2	–	2	16551.2495	3.4						16561.7649	0.1
							1	–	2	16552.3158	4.2						16562.8354	3.9
							2	–	1	16552.3568	1.1						16562.8676	–1.3
							1	–	1	16553.4230	1.8						16563.9371	1.7
							3	1	2	–	3				0	3	4	–
3	–	3	19178.0541	0.4								19086.5740	3.8					
2	–	2	19179.9629	6.0								19088.4672	3.5					

^a In MHz.^b In kHz.

position [32]. The floppy character of the NH_2 or NH group seems to be quite common in peptide molecules. It has been well established that the amide II and III modes, which are an out-of-phase and an in-phase combination of the in-plane N–H bend and the C–N stretch, respectively, reflect the characteristic feature of the peptide linkage in many biological molecules. Our calculation described above may indicate another role of vibrational spectroscopy that the N–H out-of-plane bending vibration provides us with more interesting and important information on the nature of the peptide linkage and its peripherals. As mentioned in a previous section, Suzuki [4] reported that the N–H out-of-plane bending mode appeared strongly at 720 cm^{-1} , whereas Sugawara et al. [6] analyzed the rotational structure of a band at 578.20 cm^{-1} and assigned it to the corresponding band of the *cis* form. A systematic study of the N–H out-of-plane bending band for peptides and related molecules would be worthwhile to carry out.

We have found that the deuterium isotope shifts on the potential barrier V_3 to CH_3 internal rotation were sizable for both *trans* and *cis* forms; V_3 decreased by 12 cm^{-1} in *trans* form whereas it increased by 7 cm^{-1} in *cis* form. According to our results on acetamide [15], the deuterium substitution effect in the amino group on the CH_3 internal-rotation potential may be interpreted to be due to the change in the electronic structure of the central peptide linkage. We may transfer the same mechanism to NMFA; the change in electronic structure in *trans* upon imino deuteration takes place such that the V_3 decreases, while that in *cis* makes V_3 higher.

We have demonstrated [15] that in acetamide the NH_2 wagging is coupled with the CH_3 internal rotation to produce a quite large V_6 term to the potential function of the latter. Unfortunately, we could not observe spectra of NMFA in the excited states of CH_3 internal rotation, prohibiting us from deriving the V_6 constant for this molecule. We thus examined how the V_3 potential barrier is

Table 4Molecular constants of the *trans* A state of the parent and isotopic species of NMFA and the determined r_s coordinates of heavy atoms in NMFA.^{a,b}

	<i>trans</i> A					
	Normal	H ¹³ CONHCH ₃	HC ¹⁸ ONHCH ₃	HCO ¹⁵ NHCH ₃	HCONH ¹³ CH ₃	HCONDCH ₃
A/MHz	19986.8962 (30)	19808.2778 (15)	19525.941 (11)	19667.7867 (31)	19804.4505 (12)	18359.5261 (44)
B/MHz	6405.2571 (15)	6358.0286 (17)	6135.996 (6)	6378.7686 (34)	6235.7179 (13)	6333.0344 (17)
C/MHz	4902.4309 (15)	4864.2802 (11)	4714.297 (6)	4867.7173 (21)	4791.7795 (8)	4743.9808 (19)
Δ_J /kHz	9.726 (33)	9.51 (15)	21.8 (7)	9.56 (30)	9.29 (12)	8.94 (7)
Δ_{JK} /kHz	168.22 (23)	158.24 (36)	59.8 (19)	158.7 (9)	147.54 (28)	107.85 (37)
Δ_K /kHz	634.7 (6)	634.7 ^d	634.7 ^d	634.7 ^d	634.7 ^d	369.9 (16)
δ_J /kHz	3.392 (14)	3.287 (41)	3.392 ^d	3.63 (9)	3.042 (33)	2.959 (12)
δ_K /kHz	188.5 (6)	188.5 ^d	188.5 ^d	188.5 ^d	188.5 ^d	135.8 (5)
$\Delta/u\text{Å}^2$	−1.098745 (11)	−1.1043	−1.0441	−1.1015	−1.1096	−0.7967
χ_{aa} /MHz	1.8971 (54)	1.9046 (24)	1.880 (13)	–	1.9053 (19)	1.903 (10)
$\chi_{bb} - \chi_{cc}$ /MHz	6.1744 (12)	6.1658 (48)	6.133 (27)	–	6.1705 (38)	6.277 (19)
N^c	117	38	21	8	37	88
σ /MHz	0.0120	0.0030	0.0114	0.0018	0.0024	0.0173
r_s coordinates ^e						
$a(C)/a(O)/a(N)/\text{Å}$		−0.76751	−1.33433	0.57482	1.47219	1.00839
$b(C)/b(O)/b(N)/\text{Å}$		−0.48049	0.58608	−0.64791	0.49695	−1.57463
$c(C)/c(O)/c(N)/\text{Å}$		0.05395	0.12295 i	0.03781	0.03527 i	0.41233 i

^a Derived by using ordinary asymmetric-rotor expression for the rotational energy.^b Values in parentheses denote three standard deviations given in the last digits of the constants.^c The number of transitions using in the fit.^d Assumed value.^e Calculated using Kraitchman's equation.**Table 5**Observed frequencies and their deviations from the calculated frequencies of rotational transitions of *cis* normal and N–D species of NMFA (in MHz).^a

Transition									Normal species		N-D species	
A state												
F'	J'	K'_a	K'_c	–	F''	J''	K''_a	K''_c	Obs ^b	O–C ^c	Obs ^b	O–C ^c
2	1	0	1	–	1	0	0	0	8484.2759	–3.6	8411.7317	–98.1
1	1	0	1	–	1	0	0	0	8484.9841	–0.4	8412.4485	–85.3
0	1	0	1	–	1	0	0	0	8483.2209	–1.1	8410.6856	–88.0
3	2	0	2	–	2	1	0	1	16967.1430	–1.0	16820.8923	–81.8
2	2	0	2	–	2	1	0	1	16967.9041	–2.4	16821.6549	–85.0
2	2	0	2	–	1	1	0	1	16967.1938	–7.7	16820.9507	–85.2
1	2	0	2	–	1	1	0	1	16966.0144	–1.0	–	–
1	2	0	2	–	0	1	0	1	16967.7712	–6.7	16821.5304	–74.4
3	2	1	2	–	2	1	1	1	16677.9010	4.2	16471.7973*	289.7
2	2	1	2	–	2	1	1	1	16679.2609	–0.6	–	–
2	2	1	2	–	1	1	1	1	16678.6977	4.9	16472.4010	91.1
1	2	1	2	–	1	1	1	1	16676.5730	3.1	–	–
1	2	1	2	–	0	1	1	1	16677.9938	2.1	16471.8459	151.2
3	2	1	1	–	2	1	1	0	17259.0000	0.3	17175.9172	138.5
2	2	1	1	–	2	1	1	0	17258.3863	–4.1	–	–
2	2	1	1	–	1	1	1	0	17259.6631	–1.0	17176.5805	145.6
1	2	1	1	–	1	1	1	0	17260.6116	–0.4	17177.5403	–112.4
1	2	1	1	–	0	1	1	0	17257.4314	3.7	–	–
E state												
F'	J'	K'		–	F''	J''	K''					
2	1	0		–	1	0	0		8483.2664	1.9	8411.0173	–4.7
1	1	0		–	1	0	0		8483.9739	4.4	8411.7439	17.8
0	1	0		–	1	0	0		8482.2107	3.7	8409.9525	–13.4
2	2	0		–	2	1	0		16965.8767	4.7	16820.1780	–22.9
1	2	0		–	0	1	0		16965.7488	5.5	16820.0522	–13.5
2	2	0		–	1	1	0		16965.1699	2.9	16819.4801	–16.7
3	2	0		–	2	1	0		16965.1143	4.9	16819.4167	–18.3
1	2	0		–	1	1	0		16963.9859	5.1	16818.2877	–17.8
2	2	1		–	2	1	1		16898.1658	–1.2	–	–
1	2	1		–	0	1	1		16896.6678	–15.0	16670.4057	4.0
2	2	1		–	1	1	1		16898.4059	–0.8	16672.2398	28.2
3	2	1		–	2	1	1		16897.4404	–1.4	16671.1415	7.9
1	2	1		–	1	1	1		16897.2624	–14.3	16670.7358	61.9
2	2	–1		–	2	1	–1		17036.2455*	–26.2	16973.1091	43.9
1	2	–1		–	0	1	–1		17035.4926	–30.7	16972.5826	–9.5
2	2	–1		–	1	1	–1		17036.7461	7.6	16973.6847	25.3
3	2	–1		–	2	1	–1		17036.2455	4.0	16973.3259	–9.5
1	2	–1		–	1	1	–1		17036.7461*	54.2	16974.0120	–68.1

^a The weight is reduced to 0.1 for line frequencies with *, because of inaccurate measurements for them.^b In MHz.^c In kHz.

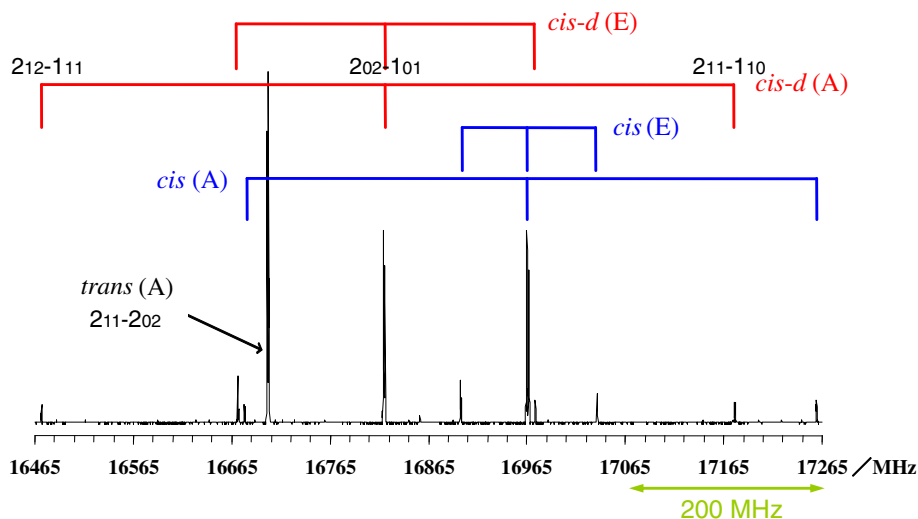


Fig. 3. Observed spectra of the $J = 2 \leftarrow 1$ transition of the *cis* normal and N-D species of NMFA.

Table 6

Molecular parameters of the *cis* normal and N-D species of NMFA.^a The rho-axis method is used.

Constant	Normal species	N-D species
A state		
A_{RAM}	43930.5 (78)	37533.89 ^b
B_{RAM}	4457.22 (14)	4464.590 (36)
C	4095.5949 (12)	4028.917 (36)
Δ_J	0.000859 (15)	0.00426 (79)
Δ_{JK}	0.00251 (15)	−0.0228 (80)
Δ_K	0.0 ^b	0.0 ^b
δ_J	0.000093 (20)	−0.0082 (11)
δ_K	0.0 ^b	0.0 ^b
E states		
A_{RAM}	43930.5 ^b	37533.89 ^b
B_{RAM}	4457.22 ^b	4464.590 ^b
C	4095.763 (44)	4028.849 (41)
Δ_J	0.000865 (20)	0.00068 (67)
Δ_{JK}	0.00353 (24)	0.0103 (71)
Δ_K	0.0 ^b	0.0 ^b
δ_J	−0.00116 (32)	−0.00347 (93)
δ_K	0.0 ^b	0.0 ^b
V_3	300.791 (48)	308.880 (42)
I_α	3.245712 ^b	3.260603 ^b
λ_a	0.999125 ^b	0.9194871 ^b
ρ	0.26077962 ^b	0.2234285 ^b
δD_E	−2.12 (54)	0.0 ^b
D_E	−1655.6 (17)	−1651.26 ^b
χ_{aa}	2.3508 (29)	2.347 (59)
$\chi_{bb} - \chi_{cc}$	6.1872 (84)	6.85 (29)
χ_{ab}	0.0 ^b	0.0 ^b
A_{PAM}	43999.81	37616.14
B_{PAM}	4387.903	4382.341
σ	0.0061	0.0785

^a In MHz, except for V_3 which is given in cm^{-1} , I_α in $\text{u}\text{\AA}^2$, and λ_a and ρ_a , which are dimensionless. Values in parentheses denote standard deviations given in the last digits of the constants.

^b Fixed; I_a was adjusted to achieve a best fit.

changed when a V_6 term is added. In order to express the effect of the V_6 term quantitatively, we introduced an index R defined by

$$R = -\left[V_3^{(6)} - V_3^{(0)}\right]/V_6 \times 100\%,$$

where $V_3^{(6)}$ denotes the value of V_3 when V_6 is added, and $V_3^{(0)}$ means the effective V_3 in absence of V_6 . The value of R is 23.0 and 18.7 for the *trans* normal and N-D species and 61.6 and 63.7 for the *cis* normal and N-D species. The R values look well correlated with

the potential functions shown in Fig. 4 and also with the deuteration effect, the latter being again opposite in sign for *trans* and *cis* forms.

4.3. Molecular structure

By combining the rotational constants of isotopomers listed in Table 4 with those of the parent species, the substitution coordinates of carbon, nitrogen, and oxygen atoms were calculated by Kraitchman's equation [33]. Here an assumption was made that the isotope variations of the second-order contributions of CH_3 internal rotation to rotational constants could be neglected. We also calculated the coordinates of the imino hydrogen using the results of Fantoni et al. [13], but the c coordinate thus obtained was found to be large and imaginary: 0.41324i \AA . We have thus reevaluated the coordinates of the imino hydrogen by using the rotational and D_E constants determined in the present study in the rho axes framework, after converting them to those in the principal inertial axes: 19455.9905, 6297.7305 and 4902.4412 MHz and 17886.770, 6204.039 and 4744.282 MHz for the *trans* normal and N-D species, respectively. The results look much more reasonable: 1.0712, 1.5241 and 0.1747 \AA .

The c coordinates of the four atoms and also of the imino hydrogen were found very close to zero or slightly imaginary, as expected from the planarity of the NMFA, and thus were set to zero in deriving molecular structure parameters given in Table 7. The r_s structure derived for the peptide linkage skeleton (i.e. a partial r_s structure) from these coordinates is listed in Table 7 along with the electron diffraction r_g and θ_α structure and with r_e parameters obtained by *ab initio* calculations for comparison.

The C=O bond length of NMFA (1.209 (3) \AA) is shorter than that in formamide [32] (1.219 (12) \AA), although the difference is marginal, whereas the C–N distance and the N–C=O angle are quite close in these two molecules: 1.353 (1) \AA and 125.0 (5)° for NMFA and 1.352 (12) \AA and 124.7 (3)° for formamide. The r_g values of three bond lengths [11]: CH_3 –N, C–N, and C=O are a little longer than the present r_s data, whereas the θ_α values of O=C–N and C–N– CH_3 are close to the present θ_s , as often found in many other molecules. The *ab initio* bond lengths are slightly longer than the present r_s values. The O=C–N–C dihedral angle of *trans* NMFA, 2.1 (5)°, is close to that in *trans* NEFA [29], 1.99 (25)°, and the O=C–N–H dihedral angle of *trans* NMFA is 176.8 (5)°. However, all the atoms in NMFA except for the two CH_3 hydrogen atoms

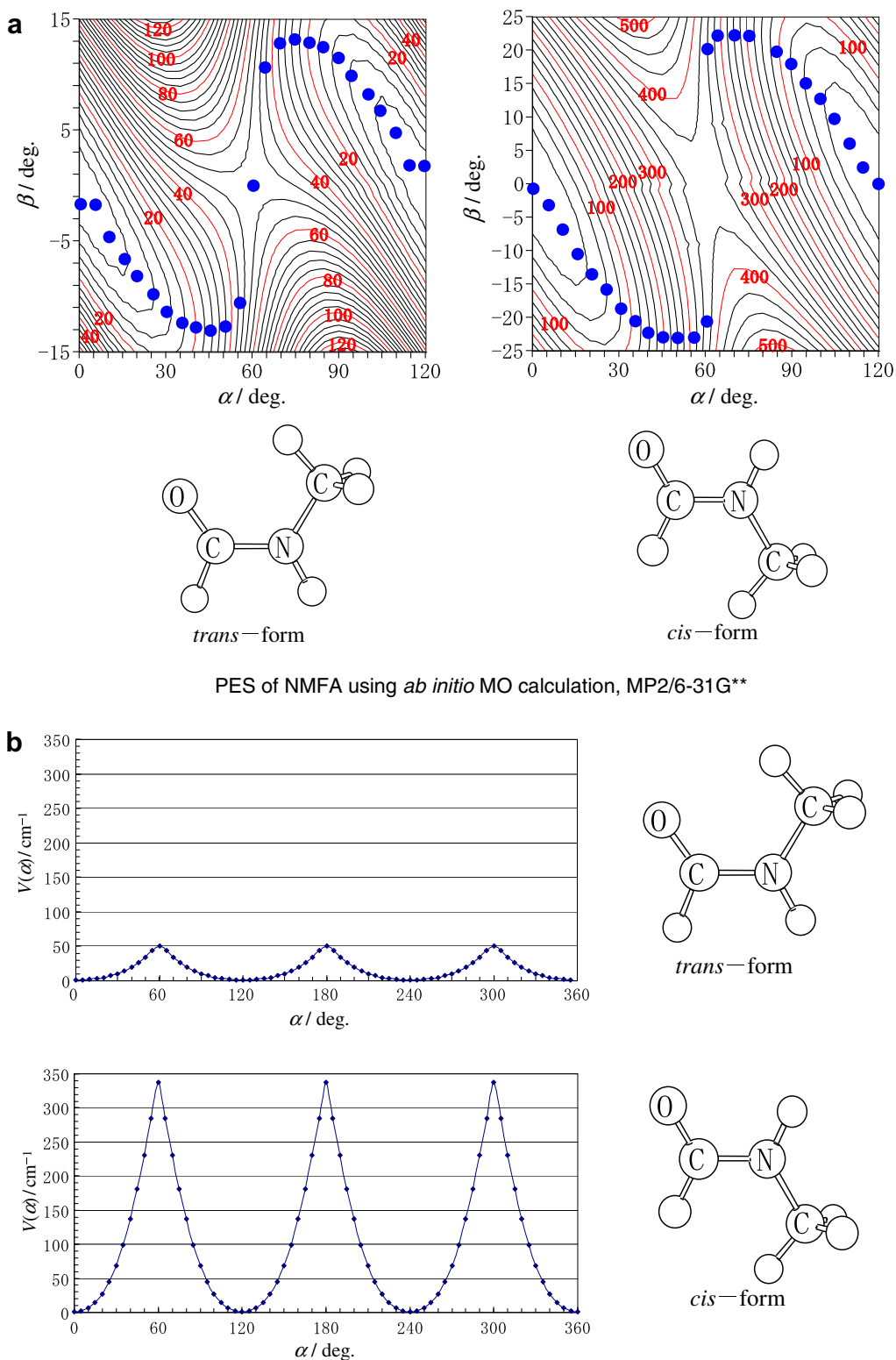


Fig. 4. (a) Potential energy function for the CH₃ internal rotation (α -axis) and N-H out-of-plane bending (β -axis) of the *trans* and *cis* forms of NMFA, calculated at the MP2/6-31G** level. The lowest-energy path is indicated by closed circles. (b) Potential energy curve as a function of the CH₃ internal-rotation angle α for the *trans* and *cis* forms of NMFA, calculated by an *ab initio* method MP2/6-31G**.

may be regarded to be in a plane, certainly the deviation from the planarity in NMFA is not as conspicuous as in the case of urea [34], in which the O=C–N–H_{*cis*} and O=C–N–H_{*trans*} dihedral angles, 10.8° and 156.9°, respectively, indicate that the amino groups are clearly pyramidal.

We have not attempted to detect spectra of *cis* isotopomers, because the spectral intensity did not seem to warrant such observations. Instead we calculated structural parameters by using the *ab initio* method described in a previous section, and the results are included in Table 7 for comparison with the corresponding structural

Table 7
Experimental and calculated structural parameters of NMFA.^a

Molecule	Trans form				Cis form	
	r_s This work	r_g Ref. [11]	r_e /DFT Ref. [36]	r_e /MP2/6-31G** This work	r_e /DFT Ref. [36]	r_e /MP2/6-31G** This work
C=O	1.209 (3)	1.219 (5)	1.233	1.228	1.232	1.226
C–N	1.353 (1)	1.366 (8)	1.357	1.361	1.360	1.362
N–CH ₃	1.455 (1)	1.459 (6)	1.455	1.449	1.453	1.446
N–H	1.019 (5)	–	1.012	1.006	1.016	1.009
/O–C–N	125.0 (4)	124.6 (5)	124.0	125.3	124.9	124.9
/C–N–CH ₃	121.0 (3)	121.4 (9)	121.3	122.3	–	124.7
/C–N–H	122.4 (10)	–	–	118.0	115.7	115.4
/O–C–N–CH ₃	2.2 (5)	–	–	0.2	–	179.7
/O–C–N–H	176.8 (5)	–	–	180.2	–	0.3

^a Bond distances and angles are given in Å and in deg, respectively.

parameters of the *trans* form. The difference between the two is not large, except for the C–N–CH₃ angle, which is larger by 2.4° in the *cis* form than in *trans* form. It is, however, interesting to note that the CH₃–N–H angle remains almost the same for the two isomers: 119.7° and 119.9° for *trans* and *cis*, respectively. The large difference in V_3 to CH₃ internal rotation in the *cis* and *trans* forms, which was clearly established in the present study, does not seem to reflect much on the skeletal structure of the NMFA molecule. This is certainly disappointing, but we may think of prosperous roles in future of internal rotation and molecular conformation in signal transfer through “molecular wire”, which can be of some significance in a variety of nano-systems such as in living things [35].

5. Conclusions

We have established that *N*-methylformamide exists in *trans* and *cis* forms with the potential barrier V_3 to CH₃ internal rotation of 53.9 and 301 cm^{−1}, respectively. The difference in V_3 between the two rotational isomers is ascribed to that in electronic structure of the central peptide linkage. The V_3 barrier changes by a large amount upon deuteration in the imino group: 41.9 and 308 cm^{−1}, respectively, namely V_3 decreased in *trans* form and increased in *cis* form by substantial amounts. The characteristic behavior of V_3 seems to be well correlated with the shape of the two-dimensional potential function for the CH₃ internal rotation versus the N–H out-of-plane bending. The V_6 term in the CH₃ internal-rotation potential function also shows some close correlation with these characteristic data.

Acknowledgments

The present study was partially supported by a Joint JSPS-NSF Grant for Cooperative Research Program. The authors are grateful to Professor Satoshi Yamamoto and Dr. E. Kim of the University of Tokyo for performing an experiment in 43 GHz region. Some of the early work was performed at NIST in Gaithersburg, Maryland when Richard Suenram was at NIST. He has since retired from NIST and is now associated with Professor Brooks Pate's Group at the University of Virginia. We greatly appreciate the support provided by NIST and all of the staff in the Optical Technology Division.

Appendix A. Supplementary data

Supplementary data for this article are available on ScienceDirect (www.sciencedirect.com) and as part of the Ohio State University Molecular Spectroscopy Archives (http://library.osu.edu/sites/msa/jmsa_hp.htm). Supplementary data associated with this article can be found, in the online version, at [doi:10.1016/j.jms.2010.06.004](https://doi.org/10.1016/j.jms.2010.06.004).

References

- [1] Y. Kawashima, T. Usami, N. Ohashi, R.D. Suenram, J.T. Hougen, E. Hirota, *Acc. Chem. Res.* 39 (2006) 216–220.
- [2] R.L. Jones, *J. Mol. Spectrosc.* 2 (1958) 581–586.
- [3] T. Miyazawa, *J. Mol. Spectrosc.* 4 (1960) 155–167.
- [4] I. Suzuki, *Bull. Chem. Soc. Jpn.* 35 (1962) 540–551.
- [5] H.E. Hallam, C.M. Jones, *Trans. Faraday Soc.* 65 (1969) 2607–2610.
- [6] Y. Sugawara, Y. Hamada, A.Y. Hirakawa, M. Tsuboi, *Chem. Phys. Lett.* 67 (1979) 186–188.
- [7] L.A. LaPlanche, M.T. Rogers, *J. Am. Chem. Soc.* 86 (1964) 337–341.
- [8] M. Liler, *J. Chem. Soc. Perkin II* (1972) 720–725.
- [9] D.E. Dorman, F.A. Bovey, *J. Org. Chem.* 38 (1973) 1719–1722.
- [10] H. Nakanishi, J.D. Roberts, *Org. Magn. Res.* 15 (1981) 7–12.
- [11] M. Kitano, K. Kuchitsu, *Bull. Chem. Soc. Jpn.* 47 (1974) 631–634.
- [12] S. Shin, A. Kurawaki, Y. Hamada, K. Shinya, K. Ohno, A. Tohara, M. Sato, *J. Mol. Struct.* 791 (2006) 30–40.
- [13] A.C. Fantoni, W. Caminati, *J. Chem. Soc., Faraday Trans.* 92 (1996) 343–346 (It should be noted that they defined the two conformations *trans* and *cis* in a way opposite to that adopted in the present study).
- [14] A.C. Fantoni, W. Caminati, H. Hartwig, W. Stahl, *J. Mol. Struct.* 612 (2002) 305–307.
- [15] E. Hirota, Y. Kawashima, T. Usami, K. Seto, *J. Mol. Spectrosc.* 260 (2010) 30–35.
- [16] V.V. Ilyushin, E.A. Alekseev, S.F. Dyubko, I. Kleiner, J.T. Hougen, *J. Mol. Spectrosc.* 227 (2004) 115–139.
- [17] J.D. Hirst, D.M. Hirst, C.L. Brooks III, *J. Phys. Chem. A* 101 (1997) 4821–4827.
- [18] T.M. Watson, J.D. Hirst, *J. Phys. Chem. A* 106 (2002) 7858–7867.
- [19] F. Hammami, M. Bahri, S. Nasr, N. Jaidane, M. Oummezzine, R. Cortes, *J. Chem. Phys.* 119 (2003) 4419–4427.
- [20] R.D. Suenram, J.-U. Grabow, A. Zuban, I. Leonov, *Rev. Sci. Instrum.* 70 (1999) 2127–2135.
- [21] Y. Kawashima, Y. Ohshima, Y. Endo, *Chem. Phys. Lett.* 315 (1999) 201–209.
- [22] S. Yamamoto, H. Habara, E. Kim, H. Nagasaka, *J. Chem. Phys.* 115 (2001) 6007–6011.
- [23] R.D. Suenram, G.Yu. Golubiatnikov, I.I. Leonov, J.T. Hougen, J. Origozo, I. Kleiner, G.T. Fraser, *J. Mol. Spectrosc.* 208 (2001) 188–193.
- [24] M.J. Frisch, G.W. Trucks, H.B. Schlegel, G.E. Scuseria, M.A. Robb, J.R. Cheeseman, V.G. Zakrzewski, J.A. Montgomery, R.E. Stratmann, J.C. Burant, S. Dapprich, J.M. Millam, A.D. Daniels, K.N. Kudin, M.C. Strain, O. Farkas, J. Tomasi, V. Barone, M. Cossi, R. Cammi, B. Mennucci, C. Pomelli, C. Adamo, S. Clifford, J. Ochterski, G.A. Petersson, P.Y. Ayala, Q. Cui, K. Morokuma, D.K. Malick, A.D. Rabuck, K. Raghavachari, J.B. Foresman, J. Cioslowski, J.V. Ortiz, A.G. Baboul, B.B. Stefanov, G. Liu, A. Liashenko, P. Piskorz, I. Komaromi, R. Gomperts, R.L. Martin, D.J. Fox, T. Keith, M.A. Al-Laham, C.Y. Peng, A. Nanayakkara, M. Challacombe, P.M.W. Gill, B.G. Johnson, W. Chen, M.W. Wong, J.L. Andres, C. Gonzalez, M. Head-Gordon, E. S. Replogle, J.A. Pople, Gaussian 09, Gaussian, Inc., Pittsburgh PA, 1998.
- [25] C. Möller, M.S. Plesset, *Phys. Rev.* 46 (1934) 618–622.
- [26] P.C. Hariharan, J.A. Pople, *Theor. Chim. Acta* 28 (1973) 213–222.
- [27] J.T. Hougen, I. Kleiner, M. Goderfroid, *J. Mol. Spectrosc.* 163 (1994) 559–586.
- [28] Y. Kawashima, R.D. Suenram, E. Hirota, *J. Mol. Spectrosc.* 219 (2003) 105–118.
- [29] K. Ohba, T. Usami, Y. Kawashima, E. Hirota, *J. Mol. Struct.* 744–747 (2005) 815–819. For *trans* form of *N*-ethylformamide and the 85th Annual Spring Meeting of the Chemical Society of Japan for *cis* form.
- [30] N. Ohashi, J.T. Hougen, R.D. Suenram, F.J. Lovas, Y. Kawashima, M. Fujitake, J. Pyka, *J. Mol. Spectrosc.* 227 (2004) 28–42.
- [31] N. Heineking, H. Dreizler, *Z. Naturforsch.* 48a (1993) 570–576.
- [32] E. Hirota, R. Sugisaki, C.J. Nielsen, G.O. Sørensen, *J. Mol. Spectrosc.* 49 (1974) 251–267.
- [33] J. Kritchman, *Am. J. Phys.* 21 (1953) 17–24.
- [34] P.D. Godfrey, R.D. Brown, A.N. Hunter, *J. Mol. Struct.* 413–414 (1997) 405–414.
- [35] Y. Kawashima, T. Usami, N. Ohashi, R.D. Suenram, J.T. Hougen, E. Hirota, in: *Symposium on Molecular Structural Basis in Creation and Transfer of Information*, Tokyo, June, 2003.
- [36] D.P. Chong, P. Aplincourt, C. Bureau, *J. Phys. Chem. A* 106 (2002) 356–362.